

TIGHT GNSS/INS INTEGRATION AS A CONSTRAINED LEAST-SQUARES PROBLEM

David Bernal, Pau Closas, Eduard Calvo, Juan A. Fernández-Rubio

Dept. of Signal Theory and Communications, Universitat Politècnica de Catalunya (UPC)
 Jordi Girona 1-3, Campus Nord, 08034 Barcelona, Spain.
 e-mail: {bernal,closas,eduard,juan}@gps.tsc.upc.edu
 http://gps-tsc.upc.es/comm2

ABSTRACT

In this paper, we study a new GNSS/INS tight integration algorithm. The underlying idea is to obtain user's position as the solution to a constrained version of the GNSS optimization problem, where classical trilateration is constrained by INS measurements. This leads to a linearly constrained least-squares problem that can be efficiently solved in worst-case polynomial time. The performance of the algorithm has been validated through simulations under challenging scenarios (namely, multipath and weak signal conditions), showing an improved performance w.r.t. GNSS stand-alone and GNSS/INS Kalman filter solutions under the same conditions.

1. INTRODUCTION

Global Navigation Satellite Systems (GNSS) is the generally concept used to identify those systems that allow user position computation based on a constellation of satellites. Specific GNSS systems are the well-known American GPS or the forthcoming European Galileo. Both systems rely on the same principle: the user computes its position from measured distances between the receiver and a set of visible satellites. These distances are calculated estimating the propagation time that transmitted signals take from each satellite to the receiver [1]. GNSS receivers are only interested in estimating delays of direct path signals, hereafter referred to as line-of-sight-signal (LOSS), as they are the ones that carry information of direct propagation time. However, reflections distort the received signal in a way that may cause a bias in delay and carrier-phase estimates [2].

To cope with this problem, the use of Inertial Navigation Systems (INS) has been widely studied in the literature to improve the position solution provided by conventional GNSS receivers [3]. An INS is a self-contained navigator that generates an attitude, position, and velocity solution. The sensors used in an INS are a triad of gyros for measuring rotation and rotation rate and a triad of accelerometers for measuring accelerations or specific force. An INS is the combination of these sensors, navigation algorithms, and the computer which hosts the algorithms.

The INS algorithms for generating attitude, position and velocity involve, in part, performing the mathematical operation of integrating the outputs of these sensors. Thus, any error on the output of the sensors leads to correlated attitude, position, and velocity errors that are potentially unbounded. A GNSS receiver, on the other hand, generates position and velocity estimates with bounded errors. Their error characteristics are complementary, being this the main reason to integrate GNSS/INS systems in many applications.

GNSS/INS integration architectures can be classified into ultra-tight, tight and loose, depending on the degree of integration between both systems [3]. An ultra-tight GNSS/INS architecture based on particle filtering was studied in [4]. The complexity of this integration approach is very high, and thus we rather focus on the other two alternatives. In tight GNSS/INS integration, the GNSS and INS are reduced to their basic sensor functions, that is, pseudorange, accelerations, and gyro measurements are used to generate a single blended navigation solution. In contrast, loose GNSS/INS integration makes the GNSS receiver and the INS operate as independent navigation systems whose positions estimates are blended to form an integrated third position solution. In general, classical tight architectures provide more accurate solutions than loose approaches [3]. Furthermore, tight integration is able to keep extracting useful information from a GNSS receiver in situations where fewer than four satellites are visible. The goal of this paper is to propose a reduced-complexity architecture that while having comparable performance to ultra-tight approaches, it is amenable from an implementation stand point. For these reasons, we concentrate on tight integration throughout the rest of the paper.

This paper is organized as follows. Section 2 introduces the system model used to describe the GNSS and INS dynamics. Section 3 provides an overview of positioning algorithms with GNSS receivers and with INS measurements, respectively. The proposed integration approach is presented in Section 4, where the constrained least-squares problem is analyzed and discussed. Section 5 focuses on simulation results that validate the proposed architecture and, finally, Section 6 concludes the paper.

2. SYSTEM MODEL

Bayesian Estimation offers an appealing framework for the joint consideration of INS measurements and GNSS pseudorange measurements. It is the natural way to ac-

This work has been financed by the Spanish/Catalan Science and Technology Commissions and FEDER funds from the European Commission: TEC2006-06481/TCM, TEC2004-04526, TIC2003-05482 and 2005SGR-00639.

count for prior information provided by the INS, which relies on a posterior probability density function to estimate a vector δ_k given the set of available measurements up to time instant k , $\mathbf{y}_{0:k}$. Besides, it is the optimal framework to deal with dynamic systems, through the discrete state-space approach. State estimates $\hat{\delta}_k \in \mathbb{R}^{n_s}$ are recursively computed given the measurements $\mathbf{y}_k \in \mathbb{C}^{n_y}$ at time index k , where n_s and n_y are the dimensions of the state and measurement vectors respectively. For that, the evolution of target states (on which measurements depend on) is modeled using a discrete-time stochastic model, the state equation, which in general reads as

$$\delta_k = \Phi_{k-1}(\delta_{k-1}, \mathbf{w}_{k-1}), \quad (1)$$

where Φ_{k-1} is a known, and possibly non-linear, function of the state δ_k and \mathbf{w}_{k-1} is referred to as process noise, which gathers any mismodeling effect or disturbances in the state characterization. The relation between the measurements and the states is modeled by the measurement equation

$$\mathbf{y}_k = \mathbf{H}_k(\delta_k, \mathbf{n}_k), \quad (2)$$

where \mathbf{H}_k is a known, and possibly non-linear function, and \mathbf{n}_k is referred to as measurement noise. Both process and measurement noise are assumed white, mutually independent, and with known statistics.

2.1 INS Data: State Equation

A 16 state vector δ is considered for tight integration. Three inertial error states are given for attitude, velocity, accelerometer bias, gyro bias, plus one state for receiver clock bias, respectively ¹:

$$\delta = \begin{bmatrix} \delta\psi^{eT} & \delta\mathbf{v}^{eT} & \mathbf{b}_a^{bT} & \mathbf{b}_g^{bT} & \delta\mathbf{p}^{eT} & \delta t \end{bmatrix}^T. \quad (3)$$

Over a sufficiently short observation period, the assumptions of non-rotating and flat Earth without gravity are valid. To remove gravity is equivalent to saying that the gravity model is perfect. The accelerometer and gyro biases, \mathbf{b}_a^b and \mathbf{b}_g^b , and the bias of the receiver clock, δt , are assumed not to have a known time variation.

Given the assumptions, the state equation (1) of the INS at time index k admits a linear approximation of the form

$$\delta_k = \Phi_{k-1}\delta_{k-1} + \mathbf{w}_k, \quad (4)$$

where Φ_{k-1} is the linearized transition matrix. At any given time instant, the specific force measured by the accelerometer, \mathbf{f}^b , and the body-to-Earth-frame coordinate transformation matrix, $\hat{\mathbf{C}}_b^e$, are used to form the transition matrix as

$$\Phi = \begin{bmatrix} \mathbf{I}_{3 \times 3} & \mathbf{0}_{3 \times 3} & \mathbf{0}_{3 \times 3} & \mathbf{0}_{3 \times 3} & \hat{\mathbf{C}}_b^e \tau_s & \mathbf{0}_{3 \times 1} \\ \Phi_{21} \tau_s & \mathbf{I}_{3 \times 3} & \mathbf{0}_{3 \times 3} & \hat{\mathbf{C}}_b^e \tau_s & \mathbf{0}_{3 \times 3} & \mathbf{0}_{3 \times 1} \\ \mathbf{0}_{3 \times 3} & \mathbf{0}_{3 \times 3} & \mathbf{I}_{3 \times 3} & \mathbf{0}_{3 \times 3} & \mathbf{0}_{3 \times 3} & \mathbf{0}_{3 \times 1} \\ \mathbf{0}_{3 \times 3} & \mathbf{0}_{3 \times 3} & \mathbf{0}_{3 \times 3} & \mathbf{I}_{3 \times 3} & \mathbf{0}_{3 \times 3} & \mathbf{0}_{3 \times 1} \\ \mathbf{0}_{3 \times 3} & \mathbf{I}_{3 \times 3} \tau_s & \mathbf{0}_{3 \times 3} & \mathbf{0}_{3 \times 3} & \mathbf{I}_{3 \times 3} & \mathbf{0}_{3 \times 1} \\ \mathbf{0}_{1 \times 3} & \mathbf{0}_{1 \times 3} & \mathbf{0}_{1 \times 3} & \mathbf{0}_{1 \times 3} & \mathbf{0}_{1 \times 3} & \mathbf{I}_{1 \times 1} \end{bmatrix}, \quad (5)$$

where $\Phi_{21} = -\left[\left(\hat{\mathbf{C}}_b^e \mathbf{f}^b\right) \times\right]$, $[\mathbf{x} \times]$ denotes the skew symmetric matrix of \mathbf{x} , and τ_s is the state propagation interval [5].

To sum up, the INS give us information on the temporal evolution of the variables of interest.

The main sources of state noise on the inertial navigation solution are random walk of the velocity error due to noise on the accelerometer specific-force measurements and random walk of the attitude error due to noise on the gyro angular-rate measurements. In addition, where separate accelerometer and gyro dynamic bias states are not estimated, the in-run time variation of the accelerometer and gyro biases can be approximated as white noise. The state noise covariance matrix, Σ_w , assuming 16 states is defined in [5].

2.2 GNSS Data: Measurement Equation

When computing the position solution, measurements are the computed pseudoranges of each visible satellite. The i -th pseudorange is obtained after estimating the travel time (τ^i) that the signal from the i -th satellite takes to reach the receiver, i.e. $\rho^i = c\tau^i$ where c is the speed of light. The pseudorange model is parameterized by the unknown user position coordinates ($\mathbf{p} = [x, y, z]^T$) and the receiver clock bias (δt) as

$$\rho^i = \varrho^i(\mathbf{p}) + c(\delta t - \delta t^i) + \epsilon^i, \quad (6)$$

where satellites are indexed by $i = 1, \dots, M$ and the following definitions apply:

- $\varrho^i(\mathbf{p}) = \sqrt{(x^i - x)^2 + (y^i - y)^2 + (z^i - z)^2}$ is the geometric distance between the receiver and the i -th satellite. $\mathbf{p}^i = [x^i, y^i, z^i]^T$ are the coordinates of the i -th satellite in the Earth-Centered Earth-Fixed (ECEF) coordinate system, which can be computed from the low-rate navigation message [1].
- δt is the bias of the receiver clock w.r.t GPS time, which is unknown.
- δt^i is the clock bias of satellite i w.r.t. GPS time, known from the navigation message.
- ϵ^i is a term that includes errors from various sources such as atmospheric delays, ephemeris mismodeling and relativistic effects among others.

The single point solution used in conventional GNSS receivers is based on the linearization of the geometrical problem consisting on the computation of \mathbf{p} and δt from a set of M estimated pseudoranges (where $M \geq 4$).

As happen with the INS, the measurement equation regarding GNSS measurements can also be linearized but now with respect to an initial estimate of the position, $\mathbf{p}_o = [x_o, y_o, z_o]^T$ as

¹where $(\cdot)^e$ denotes the e -frame and $(\cdot)^b$ denotes the b -frame.

$$\mathbf{y}_k = \mathbf{H}_k \boldsymbol{\delta}_k + \mathbf{n}_k. \quad (7)$$

Removing the time index k for the sake of simplicity, the GNSS measurements amount to

$$\mathbf{y} = \begin{bmatrix} \rho^1 + c\delta t^1 - \epsilon^1 - \varrho_o^1 \\ \vdots \\ \rho^M + c\delta t^M - \epsilon^M - \varrho_o^M \end{bmatrix}. \quad (8)$$

In turn, the structure of the measurement matrix \mathbf{H} is

$$\mathbf{H} = \mathbf{T}\mathbf{M} \triangleq \mathbf{T} \begin{bmatrix} \mathbf{0}_{4 \times 12} & \mathbf{I}_{4 \times 4} \end{bmatrix}, \quad (9)$$

where

$$\mathbf{T} = \begin{bmatrix} \frac{x^1 - x_0}{\varrho_o^1} & \frac{y^1 - y_0}{\varrho_o^1} & \frac{z^1 - z_0}{\varrho_o^1} & 1 \\ \vdots & \vdots & \vdots & \vdots \\ \frac{x^M - x_0}{\varrho_o^M} & \frac{y^M - y_0}{\varrho_o^M} & \frac{z^M - z_0}{\varrho_o^M} & 1 \end{bmatrix}. \quad (10)$$

Notice that the structure of the measurement matrix \mathbf{H} is such that, out of the complete state vector $\boldsymbol{\delta}$, only a reduced subset of variables

$$\boldsymbol{\ell} = \mathbf{M}\boldsymbol{\delta} = \begin{bmatrix} \delta \mathbf{p}^{eT} & \delta t \end{bmatrix}^T \quad (11)$$

impacts on GNSS measurements.

The measurement noise covariance matrix, $\boldsymbol{\Sigma}_n$, accounts for GNSS tracking errors, multipath variations, satellite clock noise, and residual GNSS/INS synchronization errors. It should ideally be modeled as a function of C/N_0 and acceleration, though a constant value is often assumed. The matrix $\boldsymbol{\Sigma}_n$ is diagonal, provided that the pseudo-range measurements are not carrier-smoothed [5].

3. STATE-OF-THE-ART POSITIONING ALGORITHMS

This section presents two positioning algorithms. In Section 3.1 the GNSS stand-alone solution is presented, where no use is made of INS data. In contrast, Section 3.2 sketches the conventional approach taken for GNSS/INS tight integration.

3.1 GNSS stand-alone: Least-squares

Considering only GNSS measurements, an estimate of the position can be obtained resorting to the least-squares (LS) criterion

$$\hat{\boldsymbol{\ell}}_k = \arg \min_{\boldsymbol{\ell}_k} \|\mathbf{y}_k - \mathbf{T}_k \boldsymbol{\ell}_k\|_2^2, \quad (12)$$

whose solution is given by the Moore–Penrose pseudoinverse² of the linearized matrix: $\hat{\boldsymbol{\ell}}_k = \mathbf{T}_k^\dagger \mathbf{y}_k$.

Other variants to the optimization in (12) exist which are more sophisticated. For instance, if each observation is weighted proportionally to the quality of the information provided (for instance, relating this measure with the received power), the problem can be formulated as a Weighted LS.

²We define the Moore–Penrose pseudoinverse of matrix \mathbf{T} as $\mathbf{T}^\dagger = (\mathbf{T}^H \mathbf{T})^{-1} \mathbf{T}^H$.

3.2 Tight GNSS/INS approach: Kalman filter

The discrete state-space model presented in Section 2 is linear. Therefore, it can be optimally dealt by a Kalman filter. The Kalman filter approximates the posterior pdf as Gaussian. Thus, posterior characterization is provided by its estimated mean and covariance, which are obtained recursively at each instant

$$\hat{\boldsymbol{\delta}}_{k|k-1} = \boldsymbol{\Phi}_{k-1} \hat{\boldsymbol{\delta}}_{k-1|k-1} \quad (13)$$

$$\mathbf{P}_{k|k-1} = \boldsymbol{\Sigma}_{w,k} + \boldsymbol{\Phi}_{k-1} \mathbf{P}_{k-1|k-1} \boldsymbol{\Phi}_{k-1}^T$$

$$\hat{\boldsymbol{\delta}}_{k|k} = \hat{\boldsymbol{\delta}}_{k|k-1} + \mathbf{K}_k (\mathbf{y}_k - \mathbf{H}_k \hat{\boldsymbol{\delta}}_{k|k-1})$$

$$\mathbf{P}_{k|k} = \mathbf{P}_{k|k-1} - \mathbf{K}_k (\mathbf{H}_k \mathbf{P}_{k|k-1} \mathbf{H}_k^T + \boldsymbol{\Sigma}_{n,k}) \mathbf{K}_k^T$$

where

$$\mathbf{K}_k = \mathbf{P}_{k|k-1} \mathbf{H}_k^T (\mathbf{H}_k \mathbf{P}_{k|k-1} \mathbf{H}_k^T + \boldsymbol{\Sigma}_{n,k})^{-1} \quad (14)$$

is the Kalman gain matrix.

This algorithm is the benchmark approach in tight integration of GNSS and INS data.

4. TIGHT GNSS/INS INTEGRATION AS A CONSTRAINED LEAST-SQUARES PROBLEM

In the proposed tight GNSS/INS integration algorithm, the GNSS solution (12) is enhanced by considering the evolution of the inertial measurements, but in a different way than the Kalman filter. The effect of the INS is to reduce the feasible variable space. That is, the estimate $\hat{\boldsymbol{\ell}}_k$ is now given by

$$\hat{\boldsymbol{\ell}}_k = \arg \min_{\boldsymbol{\ell}_k} \|\mathbf{y}_k - \mathbf{T}_k \boldsymbol{\ell}_k\|_2^2 \quad (15)$$

$$\text{subject to } |\boldsymbol{\ell}_k| \leq |\mathbf{M}\boldsymbol{\Phi}_k \boldsymbol{\delta}_{k-1}|. \quad (16)$$

Despite accumulated position errors provided by the INS increase exponentially in time, the errors incurred instantaneously within every integration duration are indeed bounded and small. Thus, this essentially restricts the true GNSS position error $\delta \mathbf{p}_k^{eT}$ at time index k to lie within a spatial three-dimensional cube. Similarly, the variance of the clock offset δt can be upper-bounded as well. This is represented by (16).

The problem (15)-(16) can be rewritten in the following simpler form

$$\hat{\boldsymbol{\ell}}_k = \arg \min_{\boldsymbol{\ell}_k} \|\mathbf{y}_k - \mathbf{T}_k \boldsymbol{\ell}_k\|_2^2 \quad (17)$$

$$\text{subject to } \mathbf{l}_k \leq \boldsymbol{\ell}_k \leq \mathbf{u}_k, \quad (18)$$

where \mathbf{l}_k and \mathbf{u}_k are the vectors of the lower and upper-bounds, defined as $\mathbf{l}_k = -|\mathbf{M}\boldsymbol{\Phi}_k \boldsymbol{\delta}_{k-1}|$ and $\mathbf{u}_k = |\mathbf{M}\boldsymbol{\Phi}_k \boldsymbol{\delta}_{k-1}|$. Clearly, integration takes place since the measurements \mathbf{y}_k are taken from the GNSS, while the restrictions \mathbf{l}_k and \mathbf{u}_k are obtained from the INS.

The problem (17)-(18) is a linearly constrained least-squares problem and, thus, it is convex [6]. We shall now get some intuition on the structure of $\hat{\boldsymbol{\ell}}_k$ by looking at its Karush-Kuhn-Tucker (KKT) conditions.

4.1 Interpretation

For any convex optimization problem with differentiable objective and constraint functions, a point is optimal if and only if it satisfies the KKT conditions. In particular, for the problem at hand (17)-(18) these conditions reduce to

$$\frac{\partial L(\boldsymbol{\ell}_k)}{\partial \boldsymbol{\ell}_k} = 0, \quad (19)$$

$$\lambda_{k_i} (\ell_{k_i} - u_{k_i}) = 0, \quad \lambda_{k_i} \geq 0 \quad i = \{1, \dots, \dim\{\boldsymbol{\lambda}_k\}\}, \quad (20)$$

$$\nu_{k_i} (\ell_{k_i} - \ell_{k_i}) = 0, \quad \nu_{k_i} \geq 0 \quad i = \{1, \dots, \dim\{\boldsymbol{\nu}_k\}\}, \quad (21)$$

where $L(\boldsymbol{\ell}_k)$ is the Lagrangian function

$$L(\boldsymbol{\ell}_k) = \|\mathbf{y}_k - \mathbf{T}_k \boldsymbol{\ell}_k\|_2^2 + \boldsymbol{\lambda}_k^T (\boldsymbol{\ell}_k - \mathbf{u}_k) + \boldsymbol{\nu}_k^T (\mathbf{1}_k - \boldsymbol{\ell}_k). \quad (22)$$

Thus, the optimal estimate satisfies

$$\hat{\boldsymbol{\ell}}_k = \mathbf{T}_k^\dagger \mathbf{y}_k + \frac{1}{2} (\mathbf{T}_k^T \mathbf{T}_k)^{-1} (\boldsymbol{\nu}_k - \boldsymbol{\lambda}_k), \quad (23)$$

$$\lambda_{k_i} (\delta_{k_i} - u_{k_i}) = 0, \quad \lambda_{k_i} \geq 0 \quad i = \{1, \dots, 4\}, \quad (24)$$

$$\nu_{k_i} (\ell_{k_i} - \delta_{k_i}) = 0, \quad \nu_{k_i} \geq 0 \quad i = \{1, \dots, 4\}. \quad (25)$$

From the KKT conditions, we can get some insight on the behavior of the proposed GNSS/INS integration method. Basically, three regimes of operation can be observed.

First, if the optimum unconstrained solution of the i -th element in $\boldsymbol{\ell}_k$ happens to lie between its lower and upper limits, then $\lambda_{k_i} = 0$ and $\nu_{k_i} = 0$ in order to ensure conditions in (24) and (25). In this situation, the optimum solution is calculated considering only the GNSS pseudorange, neglecting INS measurements.

Second, if the optimal unconstrained solution of the i -th element is above the constraints, $\nu_{k_i} = 0$. However, in this situation λ_{k_i} plays a role by taking on a value strictly greater than 0. Hence, the solution of the convex problem is the GNSS solution with a correction term due to the INS measurements. Analogously in the case when the optimal solution is below the lower constraint, $\lambda_{k_i} = 0$ and $\nu_{k_i} \geq 0$. Note that this is not equivalent to simply solving the unconstrained least-squares problem (12) and capping the solution using \mathbf{l}_k and \mathbf{u}_k .

Since our problem at hand is convex, strong duality holds and the optimal solution can be equivalently found as

$$\hat{\boldsymbol{\ell}}_k = \max_{\substack{\boldsymbol{\lambda}_k \geq 0 \\ \boldsymbol{\nu}_k \geq 0}} \min_{\boldsymbol{\ell}_k} L(\boldsymbol{\ell}_k; \boldsymbol{\lambda}_k, \boldsymbol{\nu}_k). \quad (26)$$

Using dual decomposition [7], we can solve (26) in an iterative manner. The resulting algorithm is described next.

Algorithm 1 Constrained least-squares

Initialize:

$$\boldsymbol{\lambda}_0 = [\mathbf{1}_{1 \times 4}]^T$$

$$\boldsymbol{\nu}_0 = [\mathbf{1}_{1 \times 4}]^T$$

for $j = 1$ to N_{iter} **do**

Initialize:

$$\beta = \frac{1+m}{j+m}$$

Compute:

$$\hat{\boldsymbol{\ell}}_k = \mathbf{T}_k^\dagger \mathbf{y}_k + \frac{1}{2} (\mathbf{T}_k^H \mathbf{T}_k)^{-1} (\boldsymbol{\nu}_j - \boldsymbol{\lambda}_j)$$

$$\boldsymbol{\lambda}_j = \left[\boldsymbol{\lambda}_{j-1} + \beta (\hat{\boldsymbol{\ell}}_k - \mathbf{u}_k) \right]^+$$

$$\boldsymbol{\nu}_j = \left[\boldsymbol{\nu}_{j-1} + \beta (\mathbf{1}_k - \hat{\boldsymbol{\ell}}_k) \right]^+$$

end for

The parameter $\beta = \frac{1+m}{j+m}$ is the step-size, and m is a non-negative integer whose value depends on the problem.

Making use of Algorithm 1, an explicit description of the procedure followed to run the proposed GNSS/INS integration during a certain period of time T_{run} is as follows

Algorithm 2 Novel tight GNSS/INS Integration

Initialize:

$$\hat{\boldsymbol{\delta}}_0 = [\mathbf{0}_{1 \times 16}]^T$$

for $k = 1$ to $\lfloor T_{run}/\tau_s \rfloor$ **do**

Initialize:

$$\hat{\boldsymbol{\delta}}_k = \boldsymbol{\Phi}_k \hat{\boldsymbol{\delta}}_{k-1}$$

$$\mathbf{u}_k = |\mathbf{M} \boldsymbol{\Phi}_k \hat{\boldsymbol{\delta}}_{k-1}|$$

$$\mathbf{l}_k = -|\mathbf{M} \boldsymbol{\Phi}_k \hat{\boldsymbol{\delta}}_{k-1}|$$

Solve $\hat{\boldsymbol{\ell}}_k$ using **Algorithm 1**.

end for

5. SIMULATION RESULTS

Although the formulation is general for any GNSS system, simulations have focused on GPS signals. The experiment has consisted in comparing the solution obtained by a GPS (i.e. equation (12)), the solution obtained when a commercial INS is integrated using Kalman filter and that obtained when a commercial INS is integrated considering the solution in Section 4. Hereafter, the former is referred to as GPS stand-alone, the second is referred to as GPS/INS Kalman, and the latter is referred to as GPS/INS constrained LS.

The performance of these algorithms was averaged over 50 realizations of a scenario consisting of 7 satellites in a realistic geometry whose carrier-to-noise ratios were 45 dB-Hz. The receiver was a vehicle with a constant velocity of 20 m/s describing a non-uniform trajectory. Pseudorange errors were computed for each satellite according to (6), where the corresponding noise term ϵ^i was drawn from $\mathcal{N}(0, \sigma_{\rho^i}^2)$ whose variance is provided by the Cramér-Rao Bound (CRB), which is the lowest error bound that any unbiased estimator can achieve. An approximation of the CRB was provided by [3] as $\sigma_{\rho^i} = \frac{c \cdot 3.44 \cdot 10^{-4}}{\sqrt{(C/N_0)_i W \tau_s}}$, where W is the filter bandwidth

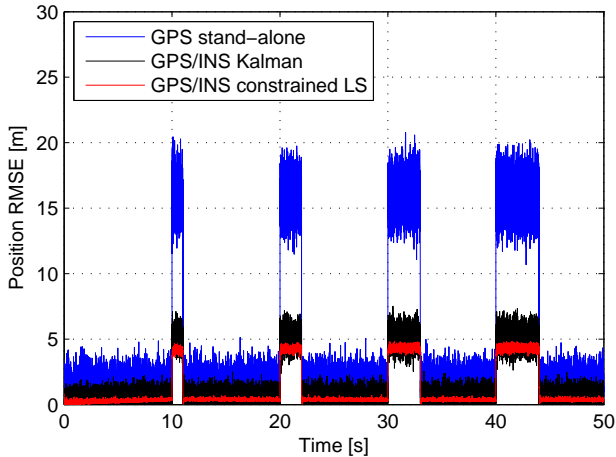


Figure 1: Multipath environment.

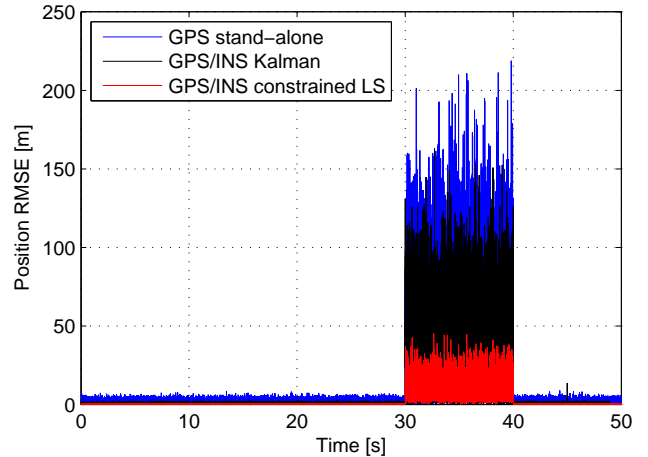


Figure 2: Satellite signal blockage during 10 s.

and τ_s the state propagation interval. The rationale of using the CRB to generate pseudorange variances was to avoid being dependent of any time-delay estimator. In particular $W = 1.1$ MHz and $\tau_s = 1$ ms. Thus, GNSS and INS measurements were available every 1 ms. The run time simulation T_{run} was fixed to 50 seconds. Parameters N_{iter} and m of algorithm 1 were set to 25 and 5, respectively.

Two challenging scenarios were considered. The first one simulated the effect of multipath, which is one of the dominant sources of error in GNSS [2]. Figure 1 shows the RMSE performance of the three positioning algorithms. Note that, whereas the GPS stand-alone solution is severely degraded, both integrated systems can cope with that situation thanks to the information delivered by the INS. Interestingly the constrained LS solution is able to improve upon Kalman filtering in both average and variance.

The second scenario simulates a satellite signal blockage ($C/N_0 = 15$ dB-Hz). This could model a vehicle driving below a bridge where there is a complete occultation of the satellites. Figure 2 shows the degradation of the stand-alone solution along with the robustness of both integrated systems. Again, the performance of constrained LS solution is better than the Kalman solution reducing the average RMSE during the occultation period from 70 to 30 meters.

6. CONCLUSIONS

An architecture for integrating GNSS receivers with INS measurements has been presented. The proposed approach is formulated as a constrained least-squares problem. A qualitative interpretation of the algorithm has been provided and an algorithm based on dual decomposition has been proposed for implementation. The proposed approach has been validated by computer simulation, where the integrated system has been compared to the performance of a GPS stand-alone receiver and the conventional GPS/INS integration using Kalman filter. Two challenging scenarios were considered: multipath and weak signal conditions.

While using the same input data as the Kalman fil-

ter the constrained least-squares uses it in a different way. Preliminary simulation results have shown performance gains that, as a subject for future work, should be verified for a wider set of scenarios.

REFERENCES

- [1] B.W. Parkinson and J.J. Spilker, Eds., *Global Positioning System: Theory and Applications*, Progress in Astronautics and Aeronautics. AIAA, Washington DC, 1996.
- [2] R. D. J. Van Nee, "Spread-Spectrum Code and Carrier Synchronization Errors Caused by Multipath and Interference," *IEEE Trans. Aerosp. Electron. Syst.*, vol. 29, no. 4, pp. 1359–1365, October 1993.
- [3] M. S. Grewal, L. R. Weill, and A. P. Andrews, *Global Positioning Systems, Inertial Navigation, and Integration*, John Wiley & Sons, 2001.
- [4] D. Bernal, P. Closas and J. A. Fernández-Rubio, "Particle Filtering Algorithm for Ultra-tight GNSS/INS Integration," Proceedings of the ION GNSS, Savannah, 2008.
- [5] D. Groves, *Principles of GNSS, inertial and multi-sensor navigation systems*, Artech House, London, England, 2008.
- [6] S. Boyd and L. Vandenberghe, *Convex Optimization*, Cambridge University Press, England, 2003.
- [7] P. Palomar and M. Chiang, "A Tutorial on Decomposition Methods for Network Utility Maximization," *IEEE Journal on Selected Areas in Communications*, vol. 24, no. 8, pp. 1439–1451, August 2006.